# Wannier exciton superradiance in a quantum-well microcavity

Gunnar Björk, Stanley Pau, Joseph Jacobson, and Yoshihisa Yamamoto*
*ERATO Quantum Fluctuation Project, Edward L. Ginzton Laboratory, Stanford University, Stanford, California 94305*
(Received 14 July 1994; revised manuscript received 7 September 1994)

Excitonic superradiance has been predicted to induce a rapid decay rate of coherently excited excitons in thin quantum wells and microspheres. In this paper we revisit this problem and derive the enhancement factor of the radiative decay due to superradiant effects. In a GaAs quantum well, the excitonic superradiant radiative decay can be roughly 320 times faster than the decay of a free electron-hole pair. The exciton decay rate depends strongly on the lateral size of the wave function when the size is smaller than the inverse of the wave vector of the emitted light. In a GaAs quantum well this corresponds to a distance of $\approx 365$ Å. Therefore, it is predicted that localization and elastic phonon scattering may lead to decay rates substantially smaller than that predicted for an ideal quantum well. It is also shown that if the quantum well is placed inside a microcavity, the decay rate can be enhanced even further since the cavity modifies the available density of radiation states in a way that matches the superradiant emission. It is predicted that in a matched dielectric cavity the decay rate can be enhanced by an additional factor of 100, but that inhomogeneous broadening may in practice limit the possible enhancement.

## I. INTRODUCTION

The dynamic response of quantum wells has been extensively studied, both experimentally and theoretically, for the last few years. Much of the incentive for these studies is the technological impact the quantum well has on quantum electronics and photonics. In spite of the advances made over the last years we feel it is safe to say that on the microscopic scale, the quantum-well exciton-field coupling is still not perfectly understood. This is in sharp contrast with two-level atomic interaction, where most of the physics was explored in the years between 1960 (the year the laser was invented) until the mid 1970s. Presently some of the ideas from that time are put to work in beautiful ways in diverse applications such as laser atom cooling, quantum noise squeezing, and Ramsey-fringe spectroscopy.

In this paper we will attack the problem of thin film superradiance, originally put forth by Lee and Lee[1] and later extended by Hanamura[2] as an explanation for the rapid decay of quantum-well excitons. Hanamura suggested that this phenomenon could account for radiative decay times as short as 2.8 ps in GaAs quantum wells. However, such short decay times have never been observed. A little later Andreani *et al.* qualitatively confirmed Hanamura's results, but predicted that the radiative decay time is 13 ps (Ref. 3) (more precisely, in the reference the exciton-field amplitude is predicted to decay in 25 ps). This estimate was later confirmed by Citrin.[4] The value also roughly coincides with the most rapid decay times measured.[5–7] In this paper we revisit the problem and extend it to include the interaction of the exciton with a single microcavity quasimode. In our model the microcavity is incorporated by a modification of the density of states. Hence the cavity mode is treated as a quasimode, and the treatment is valid for all cavity decay rates larger than the system Rabi frequency. This enables us not only to compute the temporal characteristics of the decay, but also the corresponding radiation pattern. We show that for a bare quantum well, depending on the quality and the excitation conditions, the decay rate may vary over about two orders of magnitude. More importantly, we show how the superradiant decay time can be shortened, quite substantially, by embedding the quantum well in a planar resonant microcavity. This has recently been suggested by Citrin,[8] and although our model differs substantially from that employed in (Ref. 8), we qualitatively arrive at the same results. In his analysis, Citrin employed a rather idealized model of a microcavity. In this paper we show that with some amendments, this very same idealized model cavity can in fact predict what will happen in a dielectric Bragg-mirror cavity, which is rather "leaky."[9] We show that the decay rate depends strongly on both cavity size, mirror reflectivity, and the inhomogeneous linewidth. To maximize the decay rate some optimization must be undertaken, and calculations are presented for this purpose.

In this paper we limit ourselves to predicting the purely radiative decay of Wannier excitons. Hence the photon decay rate is assumed to be sufficiently fast so that (quasi) stationary spatiotemporal exciton-polariton modes cannot form (we stay in the weak coupling regime). While other decay processes are often important in experiments, radiative decay is the major decay channel in high quality samples at low temperatures. We also limit ourselves to studying excitons that have been excited optically. Hence we exclude the nonradiative exciton-polariton modes propagating in the plane of the quantum well since, in the absence of scattering, they cannot be populated by optical excitation.

In Sec. II A a model for superradiant decay is developed. The derivation of the model relies heavily on results for two-level atom superradiance originally put forth

 

by Rehler and Eberly.[10] In the paper, the authors assume that initially the collection of atoms is completely inverted. In this work their treatment is generalized to the case when the initial excitation is small, e.g., of the order of one quanta. In this weak excitation regime (to be rigorously defined below), where phase-space filling, and hence Pauli's exclusion principle, is not important, bosonic and fermionic superradiant systems can be treated identically.[11] In Sec. III we discuss the effect of inhomogeneous broadening on the decay. In Sec. IV, the main result of this paper is presented. It is shown that the radiative decay of the quantum-well excitons should be significantly enhanced in a microcavity. In Sec. V, finally, some of our results are summarized.

## II. SUPERRADIANT DECAY

### A. Superradiant decay of two-level atoms

In this section we will adopt a model of superradiance due to Rehler and Eberly. In order to conserve space, we will omit the derivation of the model which is well described in Refs. 10 and 12. The notation in this section will closely follow that in Refs. 10 and 12. The underlying approximations Rehler and Eberly made to derive the equations below are that (1) the atoms are modeled as two-level atoms with nonoverlapping wave functions. (2) After the excitation, which is assumed to be instantaneous (e.g., by a short pulse having a wave vector $\mathbf{k}_1$), *every* atom is assumed to be in the *same* superposition of ground and upper state, i.e., the state of every atom can be described by a single number $\theta$. An alternative way of looking at this initial state is to assign a collective wave function for all the atoms. The collective wave function is essentially an atomic Bloch state. (3) Stimulated emission and absorption is assumed to be negligible. This amounts to assuming that either there is no, or little, optical feedback (i.e., the atoms and the field are in the weakly coupled regime) or the system is very weakly excited. (4) Atom-atom interaction, apart from exchange interaction, is negligible.

Following the notation of Rehler and Eberly, the total energy of the system (in units of $\hbar\omega$) following the excitation pulse is given by

$$W(t) = -\frac{N}{2}\cos\theta(t) \quad , \tag{1}$$

where $N$ is the number of atoms and $\sin^2[\theta(t)/2]$ is the probability of finding any one atom in the upper state at time $t$. The total energy $W$ is normalized in such a way that if all the atoms are in the ground state, $W = -N/2$ and if all the atoms are in the upper state then $W = N/2$. Note that $\theta$ can be interpreted as the pseudodipole tipping angle. If all atoms are inverted the pseudodipole vector points to the north pole of the Bloch sphere $\theta = \pi$ which, semiclassically, is an unstable equilibrium point. This is the initial condition in the usual treatment of atomic superradiance. We are interested in the more general case where

$$W(0) = -N/2 + x \quad , \tag{2}$$

where $x$ is the mean number of initially excited atoms.

The equation of motion for $W$ was shown by Rehler and Eberly to be

$$-\frac{dW}{dt} = \frac{\mu}{\tau_0}\left(\frac{N}{2} + W\right)\left(\frac{N}{2} - W + \frac{1}{\mu}\right) \quad . \tag{3}$$

This equation assumes that the four conditions enumerated above hold. Furthermore non-radiative decay and inhomogeneous broadening of the atoms have been neglected. In Sec. III the latter effect will be reinstated.

The parameter $\mu$ in (3) is a "shape factor" defined by

$$(1/N + \mu)I_0 = \int I_0(\mathbf{k})\Gamma(\mathbf{k}, \mathbf{k}_1)d\Omega_{\mathbf{k}} \quad , \tag{4}$$

and $I_0$ is given by

$$I_0 = \int I_0(\mathbf{k})d\Omega_{\mathbf{k}} = \hbar\omega/\tau_0 \quad , \tag{5}$$

where $I_0(\mathbf{k})$ is the radiated power per unit solid angle in the $\mathbf{k}$ direction at $t = 0$, and $\tau_0$ is the radiative decay time of an isolated atom. The energy difference between the excited and ground state is $\hbar\omega$, and $d\Omega_{\mathbf{k}}$ is the differential solid angle. The quantity $\Gamma(\mathbf{k}, \mathbf{k}_1)$ is the average phase of the far-field emission in direction $\mathbf{k}$ of the radiating atoms. It is defined by

$$\Gamma(\mathbf{k}, \mathbf{k}_1) = |\{\exp[i(\mathbf{k} - \mathbf{k}_1)\cdot\mathbf{r}]\}_{\mathrm{av}}|^2 \quad , \tag{6}$$

where the average is to be taken over the positions $\mathbf{r}$ of the atoms. Hence $\Gamma$ contains the information about how well the atomic dipole moments cooperate in the $\mathbf{k}$ direction. $\Gamma$ is unity in the directions in which the atoms all emit in phase. However, for extended samples $\Gamma$ is smaller than unity in most directions. The factor $\mu$ is usually referred to as a "shape factor" and is the integrated cooperativity over the entire solid angle weighted by the radiation pattern of the single atom. The shape factor hence contains the information on how well the atoms cooperate as a whole. For small samples in which all atoms are contained in a volume $\ll \lambda^3$ the factor is always unity since retardation effects are negligible and therefore all the atoms can radiate in phase in every direction. In larger samples $\mu$ is always smaller than unity and in order to get a smaller decay time than $\tau_0$, that is, any *super*radiance, one needs an atomic density greater than the "threshold atom density."[13] The atomic threshold density is roughly $(2\pi/\lambda)^n$, where $n = 1$ in needlelike samples, $n = 2$ in planar samples, and $n = 3$ in spherical or cubic samples. The fact that $\mu$ is smaller than unity in geometrically extended samples means that the sample operates under less than optimum cooperativity. Rehler and Eberly ascribe this effect to "a serious impedance mismatch between [the radiation modes of] free space and a geometrically large system of spontaneously emitting atoms." In Sec. IV we shall see that for planar samples it is possible to "impedance match" using a planar microcavity.

Equation (3) can be solved analytically. Inserting the initial condition (2), the solution is

$$W(t) = \frac{x(2+\mu N)\exp(-t/\tau) - N[1+\mu(N-x)]}{2[1+\mu(N-x)+\mu x\exp(-t/\tau)]} \quad . \tag{7}$$

Noting that in the absence of nonradiative decay the total emitted power $I(t)$ must equal the rate of change of the system energy, or $I(t) = -\hbar\omega dW(t)/dt$, one gets

$$I(t) = I_0 x \frac{\exp(-t/\tau)(1+\mu N)^2[1+\mu(N-x)]}{[1+\mu(N-x)+\mu x\exp(-t/\tau)]^2} \quad . \tag{8}$$

We see that only one time constant $\tau$ defined by

$$\tau = \tau_0/(1+\mu N) \tag{9}$$

is explicitly involved in the emission process, and that it is independent of $x$. In the customary treatment of superradiance this equation is solved in the limit $x \to N$. In this case (8) simplifies to

$$I(t) = I_0 N \frac{\exp(-t/\tau)(1+\mu N)^2}{[1+\mu N\exp(-t/\tau)]^2} \quad . \tag{10}$$

This is the equation derived by Rehler and Eberly in Ref. 10. It can be rewritten

$$I(t) = \frac{I_0}{4\mu}(1+\mu N)^2 \mathrm{sech}^2[(t-t_0)/2\tau] \quad , \tag{11}$$

where $t_0 = \tau \ln(\mu N)$ as shown in Ref. 10. For large values of $\mu N$, which is the typical case, the total radiation intensity at $t = 0$ is equal to $I_0 N$, i.e., there is no superradiant "enhancement" at the start of the pulse. In contrast to ordinary spontaneous emission decay, the emission intensity then grows to reach a maximum of $I_0\mu N^2/4$ at $t = t_0$. Hence the decay cannot be described by a simple exponential. It is important to note that only if $I(t)$ has a positive time derivative at $t = 0$ it is possible to have an emission power maximum at a time $t \neq 0$. Differentiating (10) with respect to time, this condition can be shown to be

$$x \geq \frac{N}{2} + \frac{1}{\mu} \quad . \tag{12}$$

Since it has already been assumed that $\mu N \gg 1$, it follows that $1/\mu \ll N$ and hence (12) above can be simplified to $x \geq N/2$.

If, on the other hand, the initial excitation is weak so that $x \ll N/2$, the decay follows an exponential law. To show this we take (8) in the opposite limit, $x \to 0$, where (8) is approximated by

$$I(t) = I_0 x\exp(-t/\tau)(1+\mu N) \quad . \tag{13}$$

We note that in this limit the pseudodipole vector is always close to the south pole of the Bloch sphere ($\theta \approx 0$). In this case, at $t = 0$, the radiative decay is enhanced by a factor of $1+\mu N$ over the case when the atoms decay independently of each other. However, as seen from (13), a monotonic exponential decay follows. It must be stressed here that this case is substantially different from the usual superradiance where the decay always starts noncooperatively. In this sense "superradiance" may be somewhat of a misnomer for this decay process, since the decay in the weak excitation limit differs fundamentally in its qualitative temporal behavior from the decay we usually associate with superradiance. On the other hand, the decay even in the weak excitation limit is a cooperative phenomenon. In this sense the term superradiance is justified. Integrating (13) over time we get the total radiated energy $E$ as

$$E = \int_0^\infty dt I_0 x\exp(-t/\tau)(1+\mu N) = I_0 x\tau(1+\mu N) = x\hbar\omega \quad , \tag{14}$$

where $I_0$ is given by (5). This confirms that our solution is self-consistent.

### B. Superradiant decay of coherently excited excitons

We shall now try to apply the theory outlined above to a system of excitons in a quantum well. The fact that the derivation above was made for a collection of two-level atoms does not play any role in the weak excitation regime where phase-space filling is negligible. We make no prediction about what will happen in the strong ($x \approx N$) excitation regime. We also note that only radiative decay has been included in the model, so interpretation of experimental results using our model must be done with caution. In order to use our theory we must compute $\mu$ and $\Gamma(\mathbf{k}, \mathbf{k}_1)$ for our sample and associate some "exciton number" with $N$ and some decay time (or matrix element) with $\tau_0$. The sample geometry we assume is depicted in Fig 1. For the time being the two mirror planes spaced a distance $L$ apart can be ig-

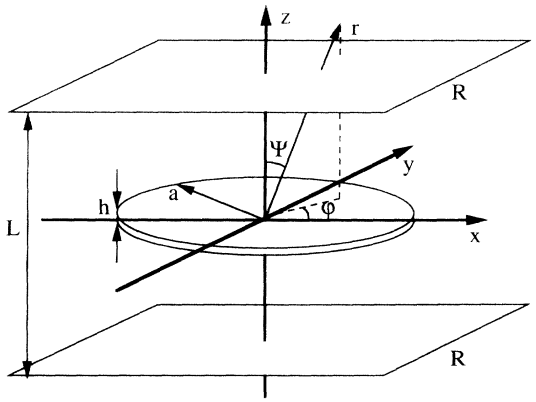


FIG. 1. Schematic drawing of the assumed geometry. The two rectangular planes represent infinitely extended mirrors forming a planar cavity. At time $t = 0$ the system is prepared by, e.g., a short light pulse in an almost plane-wave mode with $\mathbf{k}_1 \parallel \hat{\mathbf{z}}$.

nored. The quantum well is assumed to have a thickness $h \ll \lambda$ and a radius $a \gg \lambda$. The finite radius can either be due to a finite physical size of the quantum well, or associated with a finite excitation pulse beam radius, if the radius is much smaller than the lateral extent of the quantum well. The latter is usually the case in experiments. At time $t = 0$ the system is assumed to be excited by flashing a short pulse of light with constant intensity across the sample. The excitation pulse wave vector is assumed to be perpendicular to the quantum-well plane ($\mathbf{k}_1 \parallel \hat{\mathbf{z}}$), but for excitation angles not too far from the normal, the treatment below still gives a very accurate result, essentially the only change is the angle of emission. Since transverse momentum is preserved in the decay in absence of scattering, the emission will be emitted into the same directions as the quantum-well (QW) surface reflection and transmission of the excitation pulse.

As derived in Ref. 10, for a thin disk, $\mu$ can be expressed explicitly, using (4), as

$$\mu = \frac{3}{2A^2}\left(1 + \frac{\sin^2 H}{H^2}\right) \quad , \tag{15}$$

where $H = kh = 2\pi h/\lambda$ and $A = ka = 2\pi a/\lambda$. Implicitly in (15) lies the assumption that the excitation pulse wave vector is perpendicular to our quantum-well plane.

For a typical quantum well, $H \ll 1$ and $A \gg 1$. Hence the factor $\mu$ is simplified to

$$\mu \approx \frac{3}{A^2} = \frac{3}{(ka)^2} \quad . \tag{16}$$

To estimate the factor $N$, we may count the possible nonoverlapping excitonic "sites" at the same energy in the quantum well. Since $h \approx a_b$, where $a_b$ is the excitonic Bohr radius, one gets

$$N \approx \frac{\pi a^2}{\pi a_b^2} = \frac{a^2}{a_b^2} \quad . \tag{17}$$

This is effectively the number of excitons in the quantum well at the Mott density. However, due to the deformation of the exciton wave function in a quantum well, a better estimate of $N$ is[14]

$$N = \frac{8a^2}{a_b^2} \quad , \tag{18}$$

where $a_b$ is the value of the exciton Bohr radius in a bulk crystal. Before moving on we shall briefly explain why even such a crude estimate of the cooperativity number as (17) gives almost the correct result. The reason is that the superradiantly enhanced radiative decay is linked only to the size of the system wave function (the number of "unit radiators") and is independent of the excitation level, as long as $x < N/2$. Under the assumptions made, the system has only one internal degree of freedom, the excitation coordinate $W$. If the system unit radiators (e.g., two-level atoms) obey Fermi-Dirac statistics, i.e., can only accommodate one unit of excitation per unit radiator, the system is strongly nonlinear when almost all unit radiators are excited. In this limit the system will oppose additional excitation. If $x \ll N/2$, however, there are numerous unexcited unit radiators to accommodate the excitation, so that the "force" due to the Pauli exclusion principle is negligible. If, on the other hand, the unit radiators obey Bose-Einstein statistics, so that any unit radiator can accommodate any number of excitations, then the system is linear for any $x$. No "force" due to the Pauli exclusion principle exists in this system. As can be guessed from the above discussion, a system consisting of Fermi-Dirac unit radiators and a system consisting of Bose-Einstein unit radiators will behave similarly in the low excitation limit . We believe that this regime, $x \leq N/2$, is quite general for any particle-field coupling although it was derived for the specific case of superradiance. This will be the topic of future work.

At this point, it is also useful to briefly discuss cases in which there is less than optimum cooperativity. In Fig. 2 (a) we have schematically depicted an ideal quantum well, free from defects and well-width fluctuations. In such a quantum well, the exciton wave function extends over the entire area of the excited well. In real samples, however, impurities and well-width fluctuations may trap the excitons and slightly shift the exciton energy levels. However, even if the exciton is trapped locally, a coherent pulse may set up a coherent superposition of excitation over several such trapping sites. This is completely analogous to atomic superradiance where

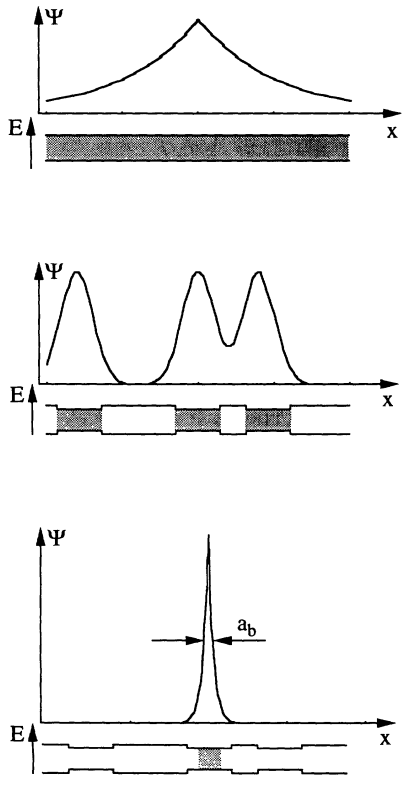


FIG. 2. Schematic drawings of the quantum-well potential function and the exciton wave function. In a perfect sample (a), the wave function extends over the entire well, whereas in (b) the excitation shows partial localization. In (c) a fully localized exciton is depicted.

each atom is distinct, but the temporal evolution may be collective. It should be stressed that the number of excited quanta in the well can be less than unity and still *cooperativity between the trapping sites will be maintained.* In this case it is a matter of convenience if one wants to describe the system as a collective motion of localized excitons, or as an extended mode with a nonmonotonic wave function [Fig. 2(b)]. The superradiant effect will be smaller in this case than in case (a), roughly in proportion to the ratio of the localization site areas to the entire excited well area. In the following we will refer to cases (a) and (b) as coherently excited superpositions of excitons, although they may equally well be called extended excitons. Finally, a truly localized exciton may emerge, i.e., as a result of phonon scattering. In principle each scattering event measures the position of an exciton and reduces the spatial extent of its wave function. After a few scattering events the exciton wave function will be extended only over small area, approaching a Bohr radius, and the radiant decay is correspondingly slower [Fig. 2(c)]. Phonon scattering leads to a temperature dependent radiative decay constant which has been observed.[15] A signature of the localized wave function is that the radiation is emitted more or less isotropically in space. This is in sharp contrast to cases (a) and (b) where, if the exciton is extended over distances larger than or equal to a wavelength, the radiation is highly directional.

To calculate the radiative enhancement rate for a weakly coherently excited superposition of excitons we use (13), (16), and (18). The result is

$$\frac{1}{\tau} \approx \frac{\mu N}{\tau_0} = \frac{6}{\pi^2}\left(\frac{\lambda}{a_b}\right)^2 \frac{1}{\tau_0} \quad , \tag{19}$$

where $\lambda$ is the transition wavelength inside the quantum well. At this point we make the identification

$$\frac{1}{\tau_0} = \frac{4ne^2\omega^3|M|^2}{3\hbar c_0^3} \quad , \tag{20}$$

where $n$ is the quantum-well refractive index, $e$ is the unit charge, and $M$ is the electron-hole transition matrix element. Hence $\tau_0$ is the radiative decay time of a free electron-hole pair, or a bulk crystal exciton. For a GaAs quantum-well Wannier exciton, the emission wavelength is about 800 nm, the refractive index is about 3.5, and $a_b \approx 100$ Å. Hence the ratio of the decay rates between an electron-hole pair and the superradiant quantum well exciton is about $\mu N = 6\lambda^2/(\pi a_b)^2 \approx 320$. Combining (19) and (20) we arrive at the decay rate

$$\frac{1}{\tau} = \frac{32e^2|M|^2\omega}{\hbar n c_0 a_b^2} \quad . \tag{21}$$

This decay rate essentially agrees with the expression derived in Ref. 2. Our rate is a factor $2/n$ smaller.

The identification of $N$ and $\tau_0$ with quantum-well parameters is somewhat arbitrary. In all cases where superradiance is important the decay rate $1/\tau$ is always proportional to $N/\tau_0$. Therefore any constant factors can in principle be incorporated either in $N$ or in $\tau_0$. The shape factor $\mu$, on the other hand, is a purely geometrical factor and is independent of the choice of the unit radiator of the system, provided that it is much smaller than a wavelength squared. An important point to notice, however, is that if only the *ratio* $N/\tau_0$ is correctly chosen, the decay rate saturation behavior for large $a$:s will always be correctly described. The only difference redistribution of constant factors between $N$ and $\tau_0$ will lead to is the behavior when $a \leq a_b$, or in more general terms, when the system dimension becomes comparable to or smaller than the unit radiator. In this limit the decay of the system is given not by the ratio $N/\tau_0$, but by $\tau_0$ alone. In atomic systems the natural assumption is that the minimum system size is that of a single atom and therefore it is natural, not to say obvious, to associate $\tau_0$ to the free space spontaneous decay rate. In an excitonic system there is not any such clear minimum system size. The interpretation of $\tau_0$ is therefore somewhat arbitrary, but for a given interpretation, there is only one corresponding choice of interpretation for $N$.

To make a connection between our theory and that in Refs. 3 and 4 we can reexpress the decay rate in the quantum-well oscillator strength per unit area $f_{2D} = 16m_0\omega|M|^2/(\pi\hbar a_b^2)$, where $m_0$ is the free electron mass. Using this expression together with (19) and (20), the expression for the decay rate is

$$\frac{1}{\tau} = \frac{2\pi e^2 f_{2D}}{n m_0 c_0} \quad . \tag{22}$$

This rate is twice as large as that derived in Ref. 3 for the longitudinal and transverse mode excitons with wave vectors close to the quantum-well plane normal. The factor of 2 discrepancy is explained by the fact that in Ref. 3, the exciton amplitude decay was computed, whereas the expression (22) refers to the decay of the energy.

The enhanced decay rate (19) is independent of the sample size as long as $a \gg \lambda/2\pi$. When this condition is fulfilled the decay rate per unit solid angle in the quantum-well normal direction is proportional to $a^2$ as shown by (25) and (27) below. One interpretation of this enhancement is that the superposition of (partially) excited excitons creates a giant dipole moment. However, as $a$ increases, the giant dipole emission will be more and more confined to angles close to the quantum-well normal. This narrowing of the radiation lobe (coupling to fewer and fewer modes of the radiation continuum) cancels the enhanced rate per solid angle (i.e., per mode) so that the emission rate saturates. To demonstrate this point we consider the spatiotemporal evolution of the radiation. The radiation intensity in the $\mathbf{k}$ direction can be written[10]

$$\begin{aligned} I(\mathbf{k},t) &= \frac{I_0(\mathbf{k})N}{2}\left\{1-\cos\theta(t)+\frac{N}{2}\sin^2\theta(t)[\Gamma(\mathbf{k},\mathbf{k}_1)-1/N]\right\} \\ &= I_0(\mathbf{k})\frac{x\mu N\exp(-t/\tau)}{2(1+\mu N)}\left(1+\frac{2N(1+\mu N)-\mu N x\exp(-t/\tau)}{2(1+\mu N)}[\Gamma(\mathbf{k},\mathbf{k}_1)-1/N]\right) \quad , \end{aligned} \tag{23}$$

where we used (1) and (7) to derive the second line. In the following we will model the "unit radiator" (essentially a localized exciton) as a dipole radiator with the dipole vector lying in the quantum-well plane. If the lateral extent of the "unit radiator" wave function is $\ll \lambda$ the radiation pattern $I_0(\mathbf{k})$ is the familiar doughnut shape

$$I_0(\varphi,\psi) = \frac{3(\cos^2\varphi + \sin^2\varphi\cos^2\psi)I_0}{8\pi} \quad , \tag{24}$$

with the emission zero in the direction of the dipole moment vector. The radiation pattern $I_0(\mathbf{k})$ is pictured in Fig. 3. The numerical factors in (24) are such that $\int I_0(\mathbf{k})d\Omega_{\mathbf{k}} = I_0$. In the case we are interested in, $x \to 0$, $\mu N \gg 1$, we can approximate (23) by

$$I(\mathbf{k},t) = \frac{I_0(\mathbf{k})\Gamma(\mathbf{k},\mathbf{k}_1)xN\exp(-t/\tau)}{2} \quad . \tag{25}$$

In addition, $\Gamma(\mathbf{k},\mathbf{k}_1)$ for a thin disk is approximately given by[10]

$$\Gamma(\mathbf{k},\mathbf{k}_1) \approx \left(\frac{\sin[H(1-\cos\psi)/2]}{H(1-\cos\psi)/2}\right)^2 \times \left(\frac{2J_1(A\sin\psi)}{A\sin\psi}\right)^2 \quad , \tag{26}$$

where $J_1$ is the first Bessel function of the first kind. One notes that for all $\psi : s$, the first factor on the right hand side of (26) is close to unity due to the smallness of $H$ (for a 100-Å-thick quantum well, using the parameters above, $H \approx 0.27$, and the first factor is larger than or equal to 0.97 for all angles), and in the second factor one can use the approximation $\sin\psi \approx \psi$ due to the largeness of $A$. Hence we get

$$\Gamma(\mathbf{k},\mathbf{k}_1) \approx \left(\frac{2J_1(A\psi)}{A\psi}\right)^2 \quad . \tag{27}$$

From this equation it is clear that $\Gamma(\mathbf{k},\mathbf{k}_1)$ and hence $I(\mathbf{k},t)$ only takes on appreciable values when $\psi$ is close to zero (or $\pi$) when $A$ is large. In Fig. 4 (27) is plotted for three values of $A$. It is seen that already for $a = \lambda$, $\Gamma(\mathbf{k},\mathbf{k}_1)$ is substantially narrower than the emission pattern of a localized exciton, Fig. 3. The full width at half maximum (FWHM) of the emission lobe is found from (27) to be approximately

$$\Delta\psi_{\mathrm{FWHM}} \approx \frac{\pi}{A} = \frac{\lambda}{2a} = \pi\sqrt{\mu/3} \quad , \tag{28}$$

where in the last step we used (16). Hence it is clear that the emission in the quantum-well normal direction is enhanced by a factor of $N \propto a^2$, but only within a solid angle proportional to $\mu \propto a^{-2}$. Therefore the total emission is enhanced by a factor proportional to $\mu N$. This must of course be the case since we already know that the system dissipates the excitation energy with the characteristic time constant $\tau_0/(N\mu)$. The continuous narrowing in the emission angle as $a$ becomes larger can be viewed as an effect of excitation delocalization. The coherent superposition of excitons becomes more and more delocalized as $a$ increases and as a consequence its transverse momentum becomes more and more well defined (centered around zero).

To see how rapidly the decay rate saturates with $a$, we have solved (4) numerically, neglecting the term $1/N$. This term is only important if $a < a_b$, and in this regime our model is not very good anyhow. In Fig. 5, $\mu$ and $\Delta\psi_{\mathrm{FWHM}}$ are plotted versus the normalized transverse size of the quantum well $a/\lambda$. The dashed line is the approximation (16). As long as $\mu$ is approximately unity, the decay rate which is proportional to $\mu N$ increases quadratically with $a$. However, when $a \geq |\mathbf{k}|^{-1}$, the shape factor $\mu$ starts to decrease as $a^{-2}$, indicating a saturation of the decay rate. In Fig. 6 we have plotted the calculated normalized radiative decay time $\tau/\tau_0$ using (9), (18), and the numerically computed value for $\mu$. It is seen that when $a/\lambda \geq (2\pi)^{-1} \approx 0.16$ the decay rate tends to the value given by (19). Hence in, e.g., a GaAs quantum well with a refractive index of 3.5, emitting at about 800 nm, the sample, or rather the radial dimen-

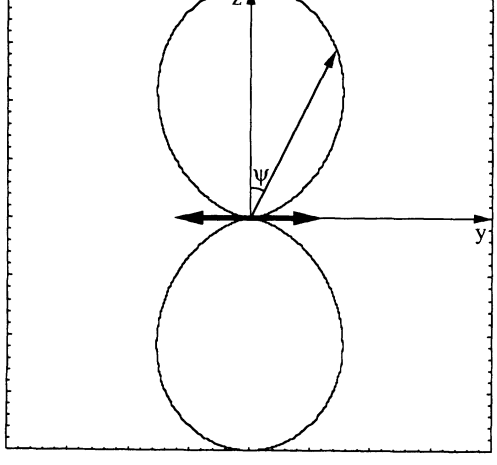


FIG. 3. The radiation pattern of a well localized dipole transition. The dipole moment vector is parallel to the $y$ axis. The radiation pattern is rotationally symmetric about the $y$ axis.

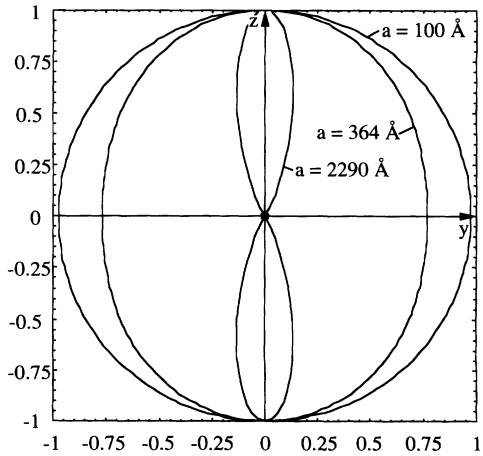


FIG. 4. Plot of the function $\Gamma$ for three values of $A$, namely, 0.275, 1, and $2\pi$, corresponding to $a = 100$ Å, $\lambda/2\pi \approx 364$ Å, and $\lambda \approx 2290$ Å.

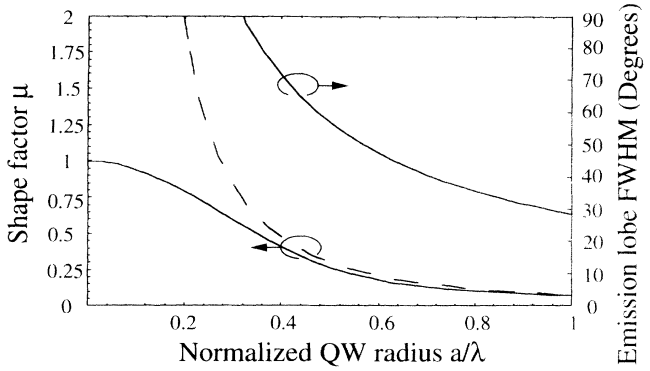


FIG. 5. The shape factor $\mu$ for a thin circular quantum-well versus the normalized quantum-well radius $a/\lambda$. The FWHM of the emission lobe is also plotted.

sion of the coherently excited superposition of excitons, must exceed 365 Å to approach the optimum decay rate. If, on the other hand, the exciton is confined to areas smaller than $\lambda/2\pi$, then the decay rate is larger than the value in (19) or (21). In Ref. 4, such effects were calculated for localization due to quantum-well monolayer thickness fluctuations. Qualitatively the results are similar to ours, but since a monolayer fluctuation only can localize an exciton weakly, the decrease in decay rate was not as dramatic as the one predicted in Fig. 6. Strong localization, due to impurity binding or dynamic localization due to repeated phonon scattering can decrease the decay rate by approximately two orders of magnitude. This may be one of the explanations that experimental data of excitonic decay rates scatter quite substantially. In Ref. 16 decay rates differing by one order of magnitude were reported for samples in which the lateral sizes of InAs quantum wells were made to differ from $\gg 100$ Å to about 35 Å. A similar scattering of the decay time (about one order of magnitude) as a function of size was also reported in Ref. 17 for excitons in CuCl microcrystals. It is worth noticing that in a good sample, an exciton created by optical excitation will initially always be sufficiently delocalized to decay at the maximum rate since essentially no light beam can be focused to a size

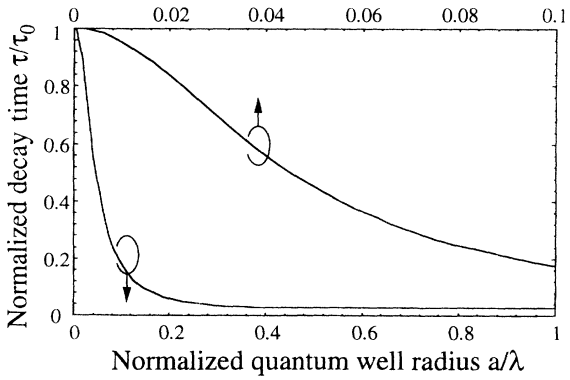


FIG. 6. The normalized radiative decay time versus the normalized quantum-well radius. The curves are the same, but they have different horizontal and vertical scales.

smaller than a wavelength squared. Therefore, in most experiments, one is operating in the regime where the superradiant decay is saturated. For the same reason, the transverse mode profile of the excitation pulse is unimportant, since any significant fluctuations across a beam take place over a lateral scale longer than a wavelength.

## III. INFLUENCE OF INHOMOGENEOUS BROADENING AND EXCITON LOCALIZATION

In Sec. II A above, the decay rate was derived assuming a homogeneously broadened exciton line. It is well known from experiments that excitonic transitions usually are accompanied by a relatively large inhomogeneous broadening mainly due to quantum-well thickness fluctuations and excitons binding to impurities. To include inhomogeneous broadening in our model, a factor $H(t)$ (not to be confused with the quantum-well normalized thickness $H = 2\pi h/\lambda$) should be included in the analysis. The inhomogeneous broadening factor is defined by[12]

$$H(t) = \frac{1}{N}\left|\sum_{l}^{N}\exp(i\Delta_l t)\right|^2 , \tag{29}$$

where $\Delta_l$ is the angular frequency detuning $\omega_l - \omega$ of the $l$th exciton site. The time evolution of $H(t)$ can be approximated by $\exp(-2|t|/T_2^*)$, where $1/T_2^*$ is the FWHM of the inhomogeneous detuning. The approximation is exact if the inhomogeneous detuning is described by a Lorentzian. To account for the inhomogeneous broadening in the system, $\mu$ in (3) and $[\Gamma(\mathbf{k},\mathbf{k}_1) - 1/N]$ in (23) should be multiplied by $H(t)$. (In Ref. 12, p. 181, it is stated that $H(t)$ should multiply only $\Gamma(\mathbf{k},\mathbf{k}_1)$ in (23). This is incorrect as the consequence would be that the decay effectively stops as soon as the excitons become dephased, and that the final state of the system is not a vacuum state $[W(t \to \infty) \neq -N/2]$.) A consequence of including $H(t)$ in (3) is that the equation can no longer be solved analytically.

Solving (3) numerically, the solution, quite expectedly, shows different behavior at times $t \ll T_2^*$ than for times $t \gg T_2^*$. At early times, before the excitons have had time to dephase appreciably, the decay is exponential, governed by the decay time $\tau = \tau_0/\mu N$. In this limit the excitonic superradiance is in full swing. At later times, when the dipoles have dephased completely due to their slightly detuned frequencies, all the superradiant enhancement of the decay has vanished, and the decay follows that of a localized exciton. The decay is still exponential but with a decay constant $\tau_0$. In between these limits there is a transient where the decay changes its rate rather abruptly, see Fig. 7. This behavior is qualitatively different from ordinary superradiant decay. In a totally inverted system the initial radiative decay is not enhanced, and therefore, if the dephasing due to inhomogeneous broadening is more rapid than the buildup of the superradiant pulse ($T_2^* < t_0$), *there will be no trace of superradiance.* In the weak excitation case treated in this paper enhanced decay will *always* be seen for times shorter than $T_2^*$. In the figure $\tau_0$ and $N$ are chosen to

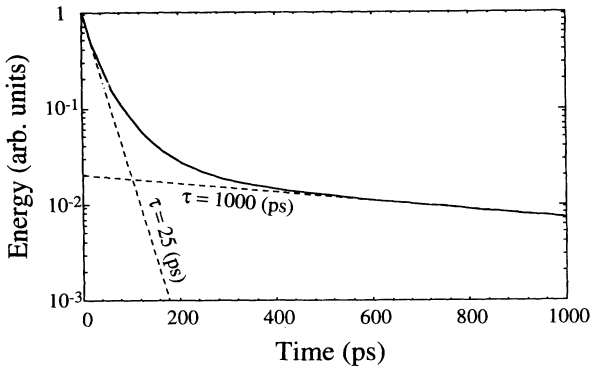


FIG. 7. The normalized total emitted radiation as a function of time. The parameters are $N = 10^6$, $\mu = 4 \times 10^{-5}$, $x = 10^3$, $\tau_0 = 1$ ns, and $T_2^* = 100$ ps. $\mu$ corresponds to a thin GaAs quantum well with $a = 10$ $\mu$m. $x$ corresponds to an exciton density of about $3 \times 10^8$ cm$^{-2}$.

model the exciton decay time going from $\tau_0/\mu N = 25$ ps to $\tau_0 = 1$ ns. Again, (19) indicates that the slowing of the radiative decay can be substantial. As in the homogeneously broadened case, the behavior outlined above is independent of $x$, as long as $x < N/2$.

The change in rate outlined above may possibly be the explanation for the results reported in Refs. 5–7 and in Ref. 17 although other explanations cannot be ruled out.[18] In these reports the authors see a rapid initial exponential decay followed by a much slower decay at later times.

## IV. SUPERRADIANCE ENHANCEMENT IN AN OPTICAL MICROCAVITY

### A. The ideal planar cavity

Now we proceed to see how a coherently excited exciton might decay in a cavity. These results must be interpreted with some caution since one of the underlying assumptions in the theory is that radiation reaction could be neglected. This condition will certainly be broken if the system is highly excited (the cavity mirrors then assure substantial optical feedback). For weak excitation and for cavity decay rates greater than the Rabi frequency the results should still be valid, however.

Most of the mathematics will remain the same even with the inclusion of the microcavity. Essentially the microcavity will only change the system "shape factor" $\mu$. To calculate the decay in this case, we take into account that the microcavity modifies the effective density of states. Hence the intensity as a function of time can be expressed

$$I(t) = \int I(\mathbf{k},t)\rho(\mathbf{k})d\Omega_{\mathbf{k}}, \tag{30}$$

where $\rho(\mathbf{k})$ is the effective density of states at the position of the quantum well in the cavity. The effective density of states is defined to be the ratio between the density of states at a given position and direction $\mathbf{k}$ in the microcavity and the density of states in the absence of cavity mirrors. If the quantum well is located in the center of a planar microcavity of length $L$ and with equal mirror reflectivity $R$ (see Fig. 1), the effective density of states $\rho(\mathbf{k})$ can be written[19,20]

$$\rho(\mathbf{k}) = \frac{(1-R)\{1+R-2\sqrt{R}\cos[|\mathbf{k}|L\cos(\psi)]\}}{(1-R)^2+4R\sin^2[|\mathbf{k}|L\cos(\psi)]} \quad , \tag{31}$$

where $|\mathbf{k}|\cos(\psi) = \mathbf{k}\cdot\hat{\mathbf{z}}$ and it has been assumed that the waves undergo a phase shift of $\pi$ upon reflection from the mirrors. In general $R$ is wavelength dependent, and furthermore, $R$ of a dielectric mirror depends on the incidence angle. Initially we will neglect both these effects and assume that $R$ is a real number such that $0 \le R \le 1$. With minor amendments this assumption is reasonable even for a dielectric mirror cavity as shall be demonstrated below. Since $\rho(\mathbf{k})$ is a local function [the expression (31) is only correct at the center of the cavity], it is not normalized as one might expect, but depends on cavity length and cavity reflectivity.[20,21] In the following it will be assumed that the microcavity is one half, or seven half wavelengths long with "cos-type" cavity modes, Fig. 8. For these specific cases one can demonstrate that

$$\int \rho(\mathbf{k})d\Omega_{\mathbf{k}} = \int_0^{\pi}\int_0^{2\pi} d\varphi d\psi \sin\psi\, \rho(\mathbf{k}) = 4\pi \quad , \tag{32}$$

independent of the mirror reflectivity. Inspection of (31) also reveals that

$$\sin\psi\, \rho(\mathbf{k}) \approx 2\pi[\delta(\psi)+\delta(\psi-\pi)] \quad \text{if } R \approx 1, \tag{33}$$

where $\delta$ is the delta function. That is, the effective density of states takes out $2\pi$ times the sum of the radiation pattern in the positive and negative $\hat{\mathbf{z}}$ direction. Figure 9 is a polar plot of the effective density of states without a cavity ($R = 0$) and for a $\lambda/2$-long microcavity with $R = 0.8$.

In addition it is useful to define the quantity $I_0'$ given by the relation

$$I_0' = \int I(\mathbf{k},0)\rho(\mathbf{k})d\Omega_{\mathbf{k}} = 2\pi\frac{2(3I_0)}{8\pi} = \frac{3I_0}{2} \quad , \tag{34}$$

where (24) and (33) have been used, and it has once

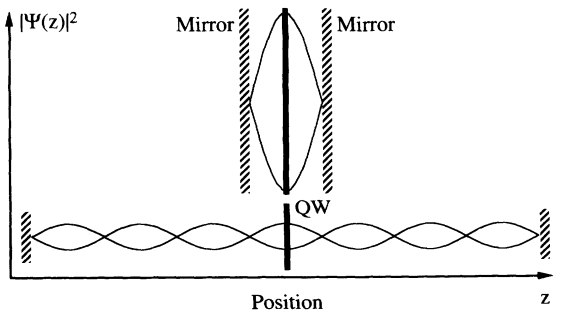


FIG. 8. A schematic drawing of a half-wavelength-long (top) and 3.5-wavelength-long (bottom) planar microcavity with "cos"-type longitudinal modes.

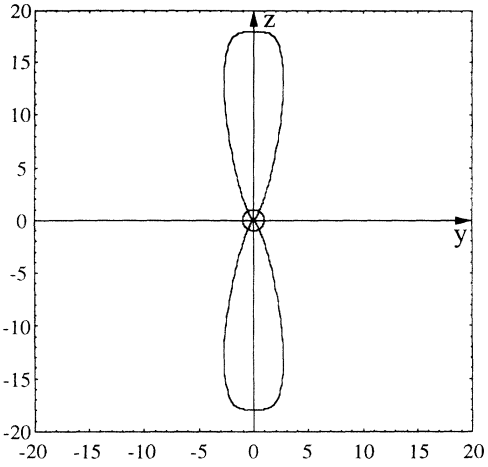


FIG. 9. The effective density of states for an ideal, half-wavelength-long microcavity with a cos-type resonant mode for $R = 0.8$. The small circle near the center is the effective density of states in the no cavity case ($R = 0$). The integrated number of modes is the same for the two curves, although it does not appear so from the plot. The reason is that the number of modes in the angular range $\psi$ to $\psi + d\psi$ is equal to $\sin\psi\rho(\mathbf{k})d\psi$.

again been assumed that the system is excited so that $\mathbf{k}_1$ is perpendicular to the quantum-well plane. It is seen that even a localized exciton in a high-finesse $\lambda/2$-long microcavity will have a shortened decay time $\tau' = 2\tau_0/3$. This is the well known microcavity spontaneous emission enhancement.[8,19–21] Finally we can write

$$\mu I_0' = -\frac{I_0'}{N} + \int I(\mathbf{k},0)\rho(\mathbf{k})\Gamma(\mathbf{k},\mathbf{k}_1)d\Omega_{\mathbf{k}} \quad . \tag{35}$$

However, in this integral $\rho(\mathbf{k})$ probes $\Gamma(\mathbf{k},\mathbf{k}_1)$ and $I(\mathbf{k},0)$ essentially only in the forward and backward directions. For small angles $\psi \ll 1/A$ and a thin quantum well, $H \ll 1$,

$$\Gamma(\mathbf{k},\mathbf{k}_1) = \frac{1}{N} + \frac{N-1}{N}\left(\frac{\sin[H(1-\cos\psi)/2]}{H(1-\cos\psi)/2}\right)^2 \times \left(\frac{2J_1(A\sin\psi)}{A\sin\psi}\right)^2 \approx \frac{1}{N} + \frac{N-1}{N} = 1 \quad . \tag{36}$$

Hence, $\mu$ can be considerably simplified by replacing $\Gamma(\mathbf{k},\mathbf{k}_1)$ by unity in (35), yielding

$$\mu = -\frac{1}{N} + \frac{1}{I_0'}\int I(\mathbf{k},0)\rho(\mathbf{k})d\Omega_{\mathbf{k}} \equiv -\frac{1}{N} + \frac{I_0'}{I_0'} = \frac{N-1}{N} \quad . \tag{37}$$

This provides the final preliminary to calculate the temporal evolution of our system. The decay in this case is still governed by (9) and (13), but in this case $1/\tau$ is given by

$$\frac{1}{\tau} = \frac{1+\mu N}{\tau'} = \frac{3(1+\mu N)}{2\tau_0} = \frac{3N}{2\tau_0} = \frac{12a^2}{\tau_0 a_b^2} \quad . \tag{38}$$

It is seen that provided the microcavity mirror reflectivity is sufficiently high, we can always overcome the restriction that excitons spatially separated by more than the inverse wave vector do not cooperate optimally (this is the "impedance mismatch problem") even if they evolve coherently. The planar microcavity couples these exciton sites to the same mode, coercing the excitons to cooperate optimally.

Equation (38) seems to indicate that there is no upper bound for the decay rate since $a$ is an unrestricted variable. This is not true, and to derive the range of validity of (38) we observe that the condition for achieving (38) is that the effective mode density $\rho(\mathbf{k})$ is a spatially "sharper" function than $\Gamma(\mathbf{k},\mathbf{k}_1)$. It can be shown[22] that the angular half-width $\Delta\psi_\rho$ (FWHM) of the normalized density of states can be expressed

$$\Delta\psi_\rho = \left(\frac{2\lambda(1-R)}{\pi L}\right)^{1/2} \quad , \tag{39}$$

where $L$ is the cavity length. In the present case $L = \lambda/2$. For $\rho(\mathbf{k})$ to be "sharper" than $\Gamma(\mathbf{k},\mathbf{k}_1)$, whose FWHM is given by (28), the condition

$$1 - R \leq \frac{\pi\lambda L}{8a^2} \tag{40}$$

must be fulfilled. However, if the excitons in the cavity are to be optically excited, we must bear in mind that when $\rho(\mathbf{k})$ is sharper than $\Gamma(\mathbf{k},\mathbf{k}_1)$, it is no longer possible to excite a circular spot which has a radius of $a$. The reason is that the cavity density of states is essentially zero for photons with wave vectors at angles greater than $\Delta\psi_\rho/2$ from the cavity normal. On the contrary, it is of course possible to optically excite an arbitrarily large spot. However, for a given reflectivity, if the spot radius $a$ is larger than that given by the condition (40), the excitons will cooperate less than optimally. Therefore in the following we will use (40) with the equality sign. This effectively means that when exciting the spot optically, (38) is only an approximation since the two functions $\rho(\mathbf{k})$ and $\Gamma(\mathbf{k},\mathbf{k}_1)$ become equally "sharp" in this case. Below we shall solve the equations numerically and show that the approximate analytical results derived in this section are essentially correct anyhow. Equating the two divergence angles (28) and (39) also effectively means that we have matched the emission to a single transverse mode of the cavity. (The cavity supports two degenerate modes with orthogonal polarization. Since the exciton emission is polarized, the excitons couple only to one of these modes.) This is an ideal situation for any optoelectronic device since matching of the emission to a single optical mode is synonymous with a 100 % radiative quantum efficiency.

Having matched the cavity to the decaying excitons in the quantum well (or vice versa), a necessary requirement to have irreversible decay is that the Rabi frequency of the system must be smaller than cavity decay rate. The Rabi (angular) frequency $\Omega_R$ can be expressed in the decay rate $1/\tau$ as

$$\Omega_R = \sqrt{\frac{2\pi c_0^3}{\omega^2 V \tau}} \quad . \tag{41}$$

where $V$ is the cavity volume. In matching the modes, we have effectively set the cavity mode radius to $a$ by assuming that the cavity reflectivity fulfills (40) with equality. (In contrast to a cavity with three-dimensional confinement the planar cavity mode volume is reflectivity dependent.[22,23]) The mode volume of our cavity can therefore be written $\pi a^2 L$. Using this relation and the expression for the decay rate (38) in (41) we arrive at

$$\Omega_R = \sqrt{\frac{6 c_0 \lambda_0^2}{\pi^2 L a_b^2 \tau_0}} \quad . \tag{42}$$

It is interesting to note that in this specific case $\Omega_R$ depends only on the cavity length whereas in the general case it depends on the cavity volume as seen in (41). This is due to our mode-matching procedure above so that the excitons only couple to a single transverse mode. Therefore only the longitudinal mode density (proportional to $1/L$) enters our expression. For a GaAs quantum well with the parameters above the Rabi (angular) frequency $\Omega_R$ is $3.6 \times 10^{13}$ s$^{-1}$ and the Rabi frequency $\Omega_R/2\pi$ is $5.7 \times 10^{12}$ s$^{-1}$. The latter value corresponds to a decay time of 175 fs.

To compute the appropriate cavity reflectivity to observe this rapid decay, we equate the Rabi frequency $\Omega_R/2\pi$ and the cavity decay rate $1/\tau_p$. The latter can be expressed[22]

$$1/\tau_p \approx \frac{c_0(1-R)}{nL} \quad . \tag{43}$$

This gives us the optimum cavity reflectivity (or rather transmittivity)

$$1 - R = \sqrt{\frac{3 n^2 L \lambda_0^2}{2\pi^3 c_0 a_b^2 \tau_0}} \quad . \tag{44}$$

For a GaAs quantum well and a half-wavelength-long cavity this leads to reflectivity of about 99% which corresponds to an excitation spot (or quantum well) radius $a$ of 1.2 $\mu$m or about five wavelengths (in GaAs).

If the quantum-well (excited spot) radius is larger than five wavelengths, the excitonic emission is more directional than the normalized density of modes for all reflectivities smaller than or equal to that given by (44). In this case $\Gamma(\mathbf{k}, \mathbf{k}_1)$ in the integral (35) will only have appreciable values very close to the forward direction. Therefore we can replace $\rho(\mathbf{k})$ in the integral by its value at $\psi = 0$ which is $(1 + \sqrt{R})/(1 - \sqrt{R})$. The decay rate becomes

$$1/\tau \approx \frac{6}{\pi^2} \left(\frac{\lambda}{a_b}\right)^2 \frac{1 + \sqrt{R}}{\tau_0 (1 - \sqrt{R})} \quad . \tag{45}$$

We shall see below that for low reflectivities the increase of the decay rate follows (45) independent of $a$. For any finite $a$, the decay rate saturates at a reflectivity given by (44) to a value given by (38) provided it is smaller than the Rabi frequency.

In Fig. 10 we have solved (35) numerically as a function of the mirror reflectivity using (26) and (31) and plotted the ensuing decay rates. To get some feeling for the numbers we have assumed that $\tau_0 = 8$ ns so that the optimal superradiant decay rate becomes 25 ps. We stress that the decay rates in the plot all scale with this number, which may be somewhat optimistic. However, the relative enhancements predicted by the analysis above are independent of $\tau_0$. The cavity decay time $\tau_p$ is also plotted and the small dashed line is Eq. (45) above. The result qualitatively agrees with those for the corresponding cavity in Ref. 8 although in that reference the decay rate was derived for a fixed reflectivity ($R = 0.95$) and with the lateral size as a variable. We see that the solid lines representing the exciton decay rate and the photon decay rate for large spots cross approximately at the Rabi frequency. This is no coincidence. Since for large pumped spot sizes the excitons only interact with one cavity mode, the decay rate and the Rabi frequency are essentially equal. It is therefore safe to say that our model holds for points where $\tau_p$ is smaller than the exciton decay time. For points to the left of the photon decay time curve, quasistationary exciton-polariton modes will appear in which the excitation energy oscillates periodically between the excitons and the field.[8,24–28] In this regime the present theory is not valid.

Furthermore, as explained above, the cavity acceptance angle given by (39) imposes a restriction on how small areas we can excite by simply focusing a coherent light beam. The cavity filters the incident excitation pulse and reflects light with incidence angles larger than the cavity acceptance angle. The maximum reflectivity

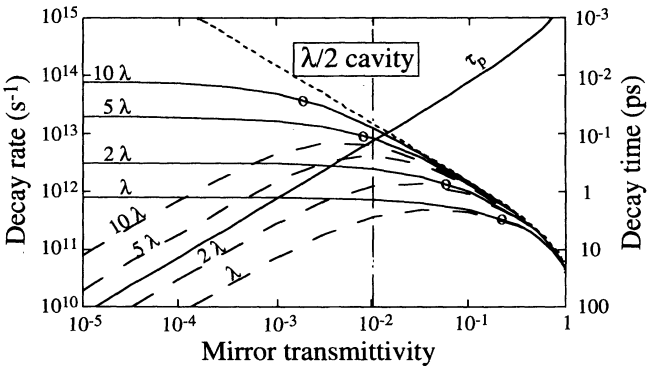


FIG. 10. The decay time as a function of the mirror reflectivity for a half-wavelength-long cavity. The cavity photon lifetime $\tau_p$ is also indicated. The circles indicate the highest reflectivity where it is still possible to form an excitation spot with the given radius by optical means. To the left of the circles the lateral exciton confinement must be achieved by other means. The dashed lines correspond to the decay time of an inhomogeneously broadened exciton transition line with a 2.5 nm linewidth. In the region to the left of the vertical dash-dotted line it is not possible to excite the entire spectral range of the exciton line due to the chromatic filtering of the cavity.

permissible for each plotted quantum-well radius $a$ has been indicated by a circle in the figure. The permissible points lie on the curve to the right of the circle. For a given cavity length and reflectivity it is of course still possible to create a coherent area smaller than the one indicated by a circle, but in this case this must be done by means other than by focusing an optical excitation pulse. The obvious way is to make the physical lateral size of the quantum-well smaller than the size given by (40). It is seen from the figure that the fastest nonreversible decay we can achieve in the assumed system is about $10^{13}$ s$^{-1}$ ($\tau = 100$ fs), which roughly coincides with the value predicted above. The corresponding reflectivity is about 0.98. Increasing the excitation radius much beyond $5\lambda$ will not make the decay substantially faster. This agrees with (45) above. We remind the reader that our predictions should be interpreted with caution since they all rely on an assumed optimum cooperativity (no exciton localization). However, using the formulas above it should be relatively easy to derive the results by scaling or recomputation for other system parameters. We should also briefly remark that although retardation effects are absent in our treatment, we believe the derived results are correct. Since the optimum decay rates are obtained coupling the cavity modes and the quantum-well excitons over distances less than ten wavelengths, retardation effects[13] should be negligible.

In real samples, the excitonic luminescence peak often has substantial inhomogeneous broadening. In the following we will assume that the broadening is due to weak localization so that the transition energy is slightly shifted from place to place within the sample. The broadening enters our calculation in two ways. First, as demonstrated in Sec. III, the dephasing with time of the corresponding exciton states will lead to a finite duration under which superradiant decay can play a role. Below it will be assumed that the inhomogeneous broadening has a half-width of 2.5 nm. This half-width corresponds to a dephasing time $T_2^*$ of about 1 ps. In this case only if the initial decay (which is what is plotted in Fig. 10) is faster than 1 ps will one see any substantial effect of superradiance. The second effect is that the cavity will act as a spectral filter for the pump pulse (which is assumed to be short and have a broad spectrum), so with increasing reflectivity, only some of the energy states within the luminescence peak will be excited. This leads to nonexcited "islands" in the quantum well, extended regions where the transition energy is larger than the energy of the transmitted excitation light. These nonexcited islands, in turn, will reduce the initial dipole moment of the coherent superposition of excitons and lead to a longer radiative decay time. In our model we include this effect through a normalized overlap integral between the cavity transmission function [which can be obtained from (31) if $|\mathbf{k}|$ is expressed in $\lambda$ or vice versa] and the inhomogeneously broadened luminescence peak, which is assumed to be a Lorentzian. The two half-widths are equal when $R = 0.99$ as indicated by the vertical dashed line in Fig. 10. The ensuing decay rates are plotted in dashed lines in the figure. It is seen that $a$ must be larger than about $2\lambda$ before the decay rate is faster than the dephasing rate. For quantum-well radii larger than about $10\lambda$ we arrive at decay rates almost as large as in the homogeneously broadened case, and most of the exciton population will decay before the excited superposition has dephased.

### B. The dielectric Bragg-mirror planar cavity

In this subsection we shall briefly discuss how our predictions are modified when a dielectric mirror microcavity is used instead of an ideal microcavity with a fixed reflectivity. The major difference between a dielectric Bragg-mirror microcavity and an ideal microcavity is that the field is less well confined in the Bragg-mirror cavity since the reflection is distributed. The field therefore penetrates into the Bragg mirror, and the effective cavity is no longer simply the physical distance between the two mirror surfaces.[29] For an epitaxial GaAs/AlAs Bragg mirror designed to be highly reflecting at 800 nm, the penetration depth is about 1.5 wavelengths, rendering a cavity with a mirror separation of half a wavelength effectively 3.0–3.5 wavelengths long. For such a cavity the effective density of states will no longer be "compressed" only into the forward and backward directions, there will also be modes at intermediate angles. In an ideal cavity these modes will be discrete, as seen in Fig. 11(a). In a Bragg-mirror cavity these modes will instead form a mode continuum in what is called the "open window."[9,19] This is pictured in Fig. 11(b), where the normalized density of states is averaged over the $S$ and $P$ polarization. The plot was computed using the method described in Ref. 9. What is important for our problem is the effective density of states in the forward and backward directions since these are the directions the superradiance preferentially couples into as manifested by Fig. 4. In the forward direction the normalized density of states function is almost identical for the dielectric and the ideal cavity, provided that the penetration depth is correctly accounted for, as seen from the figures. It can be deduced from (31) that the integrated effective density of states in the forward and backward lobe is $4\pi/7$ for a 3.5-wavelength-long microcavity. The total integrated density of states is still $4\pi$. Performing the integral (34) one finds that $I_0' \approx I_0$ in this case, and therefore the decay time constant $\tau' \approx \tau_0$. Hence the expression for the shape factor becomes

$$\mu = -\frac{1}{N} + \frac{1}{7} \quad . \tag{46}$$

The expression was derived noting that $\Gamma(\mathbf{k}, \mathbf{k}_1)$ is effectively zero everywhere but in the forward (and backward) directions, and that in the forward direction the integral over $I_0(\mathbf{k})\Gamma(\mathbf{k}, \mathbf{k}_1)$ takes out $4\pi/7$ times the value of the integrand at $\psi = 0$. Plugging this result into the expression for the decay time we arrive at

$$1/\tau = \frac{1 + \mu N}{\tau_0} \approx \frac{N}{7\tau_0} = \frac{8a^2}{7\tau_0 a_b^2} \quad . \tag{47}$$

We see that this predicted decay rate is about an order

of magnitude smaller in a dielectric Bragg-mirror microcavity than in an ideal, half-wavelength-long microcavity. A decrease is to be expected since the photons are less well localized in the dielectric microcavity than in the ideal cavity. Therefore the transition matrix element becomes weaker. In our treatment this effect has been incorporated through the effective density of states. However, the real limitation to the decay rate is given by the Rabi frequency, and as shown above, it scales as $L^{-1/2}$. Hence we should expect that in a dielectric microcavity the fastest observable decay rate should be roughly $1/\sqrt{7} \approx 0.38$ times that in an ideal half-wavelength-long microcavity. This is confirmed by Fig. 12 where we have solved the relevant equations for a 3.5-wavelength-long microcavity and plotted the decay rates. It is seen that the "optimum" decay rate in this case is about $5 \times 10^{12}$ $s^{-1}$ (or $\tau = 200$ fs) and that the minimum quantum-well radius to achieve this rate is about $10\lambda$ in this case. One should also note that in this case the mirror reflectivity must not exceed 0.95 in order to see irreversible decay. High-finesse, high quality samples should exhibit

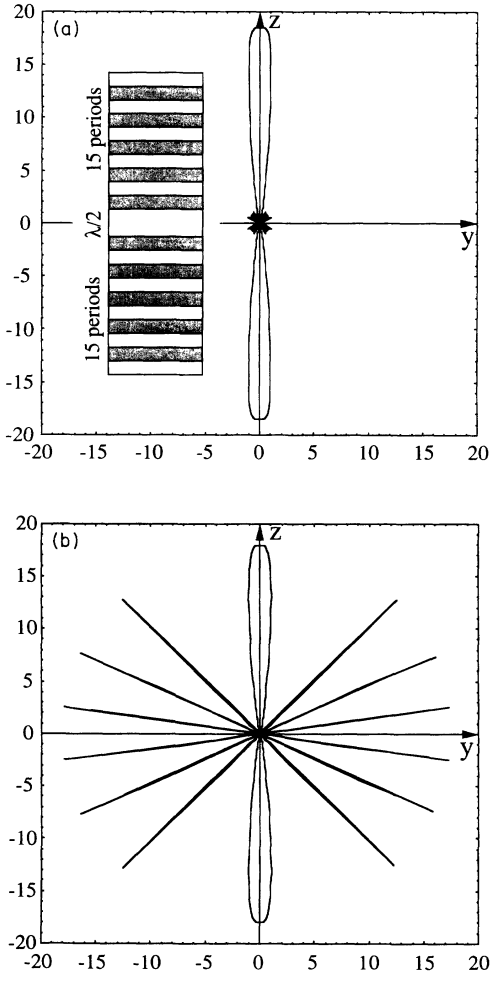


FIG. 11. The effective density of states for a Bragg-mirror microcavity (the structure is shown in the inset) is shown in (a), and for a 3.5-wavelength-long cavity with ideal mirrors in (b).

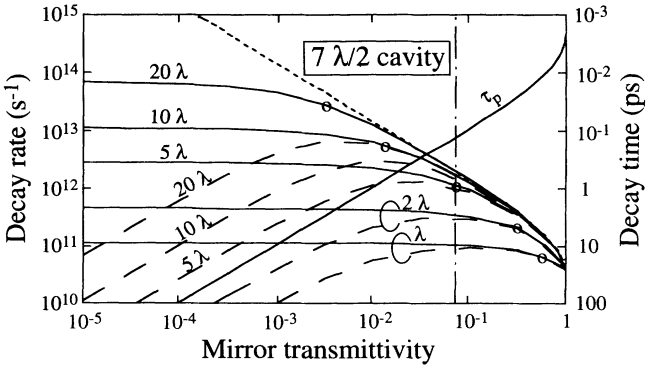


FIG. 12. The decay time as a function of the mirror reflectivity for a 3.5-wavelength-long cavity. The nomenclature and parameters are the same as in Fig. 10.

reversible decay. This is confirmed by recent reports of exciton-polariton normal mode splitting in GaAs quantum wells.[24,26–28]

It is worth pointing out two final things regarding superradiant excitonic decay in dielectric planar cavities. The first is that, as demonstrated above, the planar dielectric cavity is not optimal due to the finite mirror penetration depth. This fact notwithstanding, it is still possible to increase the decay rate by about two orders of magnitude over the ordinary superradiant decay. Secondly, the half-wavelength-long planar microcavity is an *optimum* cavity to enhance the decay rate of a coherent superposition of excitons. This particular cavity realizes the full cooperativity of the exciton superposition states in the quantum well. This is in sharp contrast to the enhancement of the radiative decay of free electron-hole pairs, where the decay rate only can be enhanced by a modest factor of 3 by a planar cavity. A dielectric planar cavity hardly enhances the rate of free electron-hole pair radiative decay at all.[8,20–22] This shows that the full potential of the planar cavity is harnessed only by extended excitations which match the cavity mode, not by point excitations.

## V. CONCLUSIONS

We have shown that excitonic superradiance of Wannier excitons in a quantum well can be described using a model originally developed for two-level atom superradiance when the excitation density is much smaller than about half the Mott density. In this regime the decay is purely exponential in time. The reason one can treat two fundamentally different systems (one essentially boson-boson coupling, the other fermion-boson) with the same model is that the physics of the problem at low excitation lies in the geometry, not in the commutation relations. The standard view of excitonic superradiance is that the wave function of every exciton is extended over the whole coherently excited area. In this paper it is shown that an equivalent view is to assume that every exciton "site" in the quantum well is partially excited. An advantage with

our treatment is that it naturally incorporates the coupling with the free space mode continuum and therefore gives information about the radiation pattern.

Using the model we show that collective behavior of a coherent superposition of excitons, or "excitonic superradiance," will indeed shorten the decay time considerably compared to the decay time of a free electron-hole pair. In thick (150-200 Å) GaAs quantum wells the optimum decay rate of the Wannier excitons is about 320 times larger than that of a free electron-hole pair. Our expression for the decay time agrees exactly with that of Andreani *et al.*[3]

The effect of inhomogeneous broadening is also discussed. It is predicted that excitonic superradiance will only be seen in high quality samples. In low quality samples the excitons will dephase before any significant superradiant decay has had time to come into play. However, even in high quality samples, two distinctly different decay times are predicted to be seen, a rapid decay for times short compared to the inverse of the inhomogeneous linewidth, and a slower decay at longer times. This prediction qualitatively agrees with recent measurements.

Finally, and most importantly, it is shown that the decay rate (or equivalently, the exciton-field coupling) can be increased by at least an additional two orders of magnitude by embedding the quantum well in an optimized planar microcavity. If one tries to increase the decay rate beyond the optimum valu- one enters the regime of (quasi) stationary exciton-pola iton normal modes which decay slowly. The effect of the microcavity is to redistribute the effective density of states in such a way as to "impedance match" the superradiant excitons to free space. This is an exciting finding that may be used in future high-speed high-quantum-efficiency optoelectronic devices.

## ACKNOWLEDGMENTS

The authors would like to thank Professor E. Hanamura for helpful comments. We are also indebted to Dr. D. Citrin for enlightening discussions, and for sharing unpublished material (Ref. 8) with us. S.P. gratefully acknowledges financial support from the John and Fannie Hertz Foundation.

---

* Also at NTT Basic Research Laboratories, Atsugishi, Kanagawa, Japan.

[1] Y. C. Lee and P. S. Lee, Phys. Rev. B **10**, 344 (1974).
[2] E. Hanamura, Phys. Rev. B **38**, 1228 (1988).
[3] L. C. Andreani, F. Tassone, and F. Bassani, Solid State Commun. **77**, 641 (1991).
[4] D. S. Citrin, Phys. Rev. B **47**, 3832 (1993).
[5] B. Sermage, B. Deveaud, K. Satzke, F. Clérot, C. Dumas, N. Roy, D. S. Katzer, F. Mollot, R. Planel, M. Berz, and J. L. Oudar, Superlatt. Microstruct. **13**, 271 (1993).
[6] B. Deveaud, F. Clérot, N. Roy, K. Satzke, B. Sermage, and D. S. Katzer, Phys. Rev. Lett. **67**, 2355 (1991).
[7] B. Deveaud, F. Clérot, N. Roy, B. Sermage, and D. S. Katzer, Surf. Sci. **263**, 491 (1992).
[8] D. S. Citrin, IEEE J. Quantum Electron. **30**, 997 (1994); D. S. Citrin, Opt. Soc. Am. Tech. Dig. Ser. **9**, 114 (1994).
[9] G. Björk, Y. Yamamoto, S. Machida, and K. Igeta, Phys. Rev. A **44**, 669 (1991).
[10] N. E. Rehler and J. H. Eberly, Phys. Rev. A **3**, 1735 (1971).
[11] G. S. Agarwal, J. Opt. Soc. Am. B **2**, 480 (1985).
[12] L. Allen and J. H. Eberly, *Optical Resonance and Two-level Atoms* (John Wiley & Sons, New York, 1975).
[13] F. T. Arecchi and E. Courtens, Phys. Rev. A **2**, 1730 (1970).
[14] M. Shinada and S. Sugano, J. Phys. Soc. Jpn. **21**, 1936 (1966).
[15] B. Zhang, Y. Shiraki, and R. Ito, J. Phys. Soc. Jpn. **63**, 358 (1994).
[16] O. Brandt, G. C. La Rocca, A. Heberle, A. Ruiz, and K. Ploog, Phys. Rev. B **45**, 3803 (1992).
[17] T. Itoh, M. Furumiya, and T. Ikehara, Solid State Commun. **73**, 271 (1990).
[18] H. Wang, J. Shah, T. C. Damen, and N. L. Pfeiffer (unpublished).
[19] Y. Yamamoto, S. Machida, K. Igeta, and G. Björk, in *Coherence, Amplification, and Quantum Effects in Semiconductor Lasers*, edited by Y. Yamamoto (Wiley Interscience, New York, 1991).
[20] G. Björk, IEEE J. Quantum Electron. **30**, 2314 (1994).
[21] S. D. Brorson, H. Yokoyama, and E. Ippen, IEEE J. Quantum Electron. **26**, 1492 (1990).
[22] G. Björk, H. Heitmann, and Y. Yamamoto, Phys. Rev. A **47**, 4451 (1993).
[23] K. Ujihara, Jpn. J. Appl. Phys. **30**, L901 (1991).
[24] C. Weisbuch, M. Nishioka, A. Ishikawa, and Y. Arakawa, Phys. Rev. Lett. **69**, 3314 (1992).
[25] Y. Yamamoto, F. Matinaga, S. Machida, A. Karlsson, J. Jacobson, G. Björk, and T. Mukai, J. Phys. IV (France) **3**, 39 (1993).
[26] R. Houdré, R. P. Stanley, U. Oesterle, M. Ilegems, and C. Weisbuch, J. Phys. IV (France) **3**, 51 (1993).
[27] C. Norris, J.-K. Rhee, C. Y. Sung, Y. Arakawa, M. Nishioka, and C. Weisbuch (unpublished).
[28] J. Jacobson, H. Cao, S. Pau, G. Björk, and Y. Yamamoto (unpublished).
[29] D. I. Babic and S. W Corzine, IEEE J. Quantum Electron. **28**, 514 (1992).

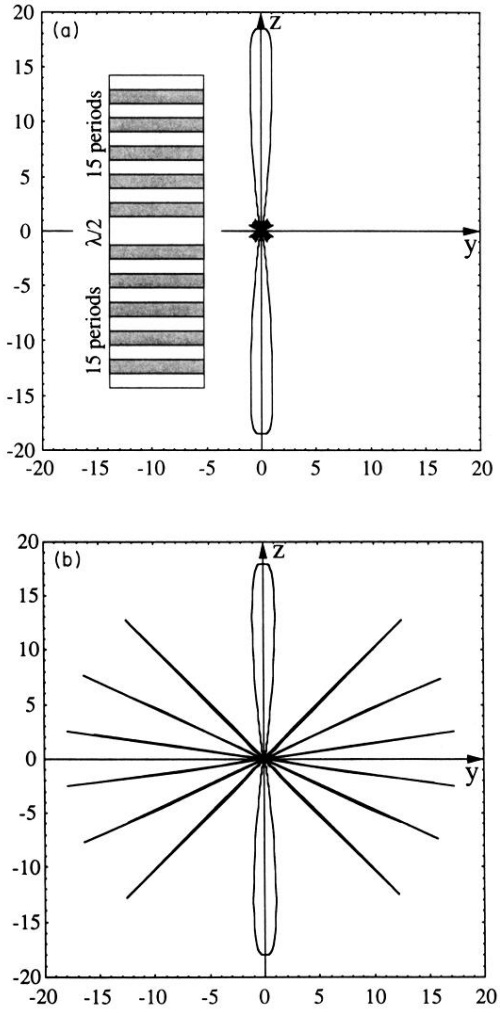


FIG. 11. The effective density of states for a Bragg-mirror microcavity (the structure is shown in the inset) is shown in (a), and for a 3.5-wavelength-long cavity with ideal mirrors in (b).

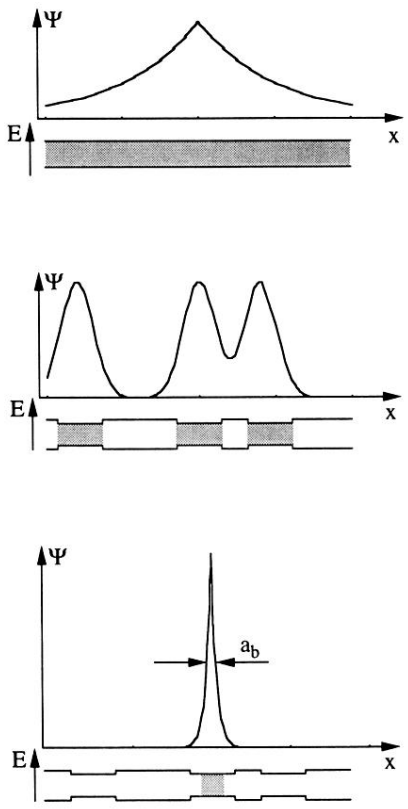


FIG. 2. Schematic drawings of the quantum-well potential function and the exciton wave function. In a perfect sample (a), the wave function extends over the entire well, whereas in (b) the excitation shows partial localization. In (c) a fully localized exciton is depicted.